J. Membrane Biol. 165, 235–242 (1998)

The Journal of
Membrane
Biology

Simple Carrier Kinetics in Complex Membrane Transporters

J.A. Hernández
Sección Biofisica, Facultad de Ciencias, Universidad de la República, 11400 Montevideo, Uruguay

Received: 9 February 1998/Revised: 19 June 1998

Abstract. The four-state simple carrier model (SCM) has been employed to describe facilitative transport of ligands across biological membranes. Two basic mechanisms have been invoked to account for carrier-mediated ligand translocation: (i) binding to a mobile carrier, and (ii) displacement determined by conformational changes of an integral protein. While translatory carriers may be accurately represented by a four-state diagram, it is unlikely that the transport process mediated by a complex membrane protein can be strictly described by the elementary SCM. The purpose of this article is to test whether facilitative transporters with a more complex kinetic design than the SCM can exhibit macroscopic kinetic properties indistinguishable from it. For this, I studied a ''general carrier model'' (GCM), and evaluated whether the relevant kinetic parameters are subject to the same basic restrictions as in the SCM. The fundamental finding is that there is a general kinetic design embodied with SCM-like properties, that can be shared by many transporters. In particular, the classical SCM is shown here to represent a particular case of the GCM. A main conclusion of this work is therefore that the finding of a macroscopic SCM-like kinetic behavior for a particular process of facilitative transport does not represent a sufficient argument in favor of a particular type of mechanism, like the typical one involving a two-conformational single-site carrier.

Key words: Carriers — Transporters — Kinetic models — Membrane transport

Introduction

The processes of mediated transport across membranes play crucial roles in cellular physiology. They usually are accomplished by complex integral membrane proteins that translocate ionic or nonionic ligands between the compartments separated by the membrane. Two basic kinetic forms of mediated transport have classically been distinguished: channel and carrier. The four-state model (Fig. 1) represents the most elementary scheme to describe the kinetics of facilitated diffusion mediated by carriers (Schultz, 1980; Stein, 1986; Andersen, 1989). This ''simple carrier model'' (SCM) accounts for the two basic mechanisms invoked for carrier kinetics: (i) ligand translocation by a lipid-soluble mobile carrier, and (ii) internal site displacement determined by conformational changes of an integral protein. While translatory carriers of the valinomycin type may be accurately represented by a four-state diagram, it is unlikely that the transport process mediated by a complex integral membrane protein can be strictly described by the elementary SCM. An example of SCM-like behavior exhibited by a complex transporter is provided by the facilitative glucose transporter (Walmsley, 1988; Carruthers, 1990; Baldwin, 1993; Gould & Holman, 1993). In this case, strict application of the SCM results controversial, since the totality of the experimental results cannot be explained by a single SCM (Stein, 1986; Wheeler & Whelan, 1988; Carruthers, 1990). This fact might be revealing that a process more complex than the one represented by Fig. 1 is taking place. In previous work (Hernández, Fischbarg & Vera, 1996) we demonstrated that a more involved mechanism, corresponding to a two-conformational two-site channel, could exhibit SCM-like properties under a single-occupancy regime and a more complex behavior under higher occupancies of the ligand. Hence, the mechanism was proposed as a plausible alternative to interpret the controversial kinetic behavior of the glucose transporter. The glucose transporter thus constitutes an example that the SCM-like behavior can be exhibited by complex transporters, sometimes characterized by kinetic diagrams not immediately suggestive of that type of behavior. Other ex-

Correspondence to: J.A. Hernández

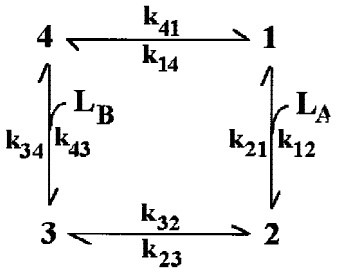

Fig. 1. State diagram of the simple carrier model. 1, . . . , 4 are the intermediate states of the carrier. L_A and L_B represent the ligand, binding from compartments *A* and *B* respectively. The *k*s represent the true rate constants, governing the corresponding transitions.

amples of complex membrane transporters exhibiting SCM-like kinetics are, for instance, the choline transporter (Krupka & Deves, 1981, 1983) and diverse aminoacid transporters (for references, *see* Stein, 1990).

The purpose of this article is to test whether facilitative transporters with a more complex kinetic design than the SCM can nevertheless exhibit macroscopic kinetic properties indistinguishable from it. For this, I studied a ''general carrier model,'' and evaluated whether the relevant kinetic parameters are subject to the same basic restrictions as in the SCM. The basic results from the analysis of this general carrier model is that the relevant experimental parameters determining the macroscopic behavior are in effect subject to the same kinetic restrictions as in the SCM. Therefore, the fundamental finding of this study is that there is indeed a general kinetic design embodied with SCM-like properties, that can be shared by a great variety of transporters. This general design determines the necessary and sufficient structural features of the kinetic diagram of the transporter that in turn determine the SCM-like macroscopic behavior.

Results and Discussion

The Simple Carrier Model

The kinetic characterization of the simple carrier has been performed by Lieb and Stein (1974; *see also* Stein, 1986). As a reference for the rest of the work, I reproduced the basic aspects of their approach here.

For the model shown in Fig. 1, the unidirectional fluxes v_{AB} and v_{BA} (in the $A \rightarrow B$ and $B \rightarrow A$ directions, respectively) are given by

$$v_{AB} = (K + L_B)L_A/\Sigma \text{ and } v_{BA} = (K + L_A)L_B/\Sigma, \qquad (1a)$$

with

$$\Sigma = K^2 R_{00} + K R_{AB} L_A + K R_{BA} L_B + R_{ee} L_A L_B \qquad (1b)$$

The net flux J_L (positive in the $A \rightarrow B$ direction) is given by

$$J_L = v_{AB} - v_{BA} \qquad (1c)$$

In Eqs. (1), L_A and L_B are the ligand (L) concentrations in compartments *A* and *B* respectively, and K, R_{00}, R_{AB}, R_{BA} and R_{ee} are the relevant experimental parameters given, for the case of the SCM shown in Fig. 1, by

$$K = (k_{14}/k_{12}) + (k_{41}/k_{43}) + [k_{34}\, k_{41}/(k_{43}\, k_{32})]$$

$$N\, R_{AB} = (1/k_{34}) + (1/k_{41}) + (1/k_{23}) + [k_{32}/(k_{23}\, k_{34})]$$

$$N\, R_{BA} = (1/k_{21}) + (1/k_{14}) + (1/k_{32}) + [k_{23}/(k_{32}\, k_{21})] \qquad (2)$$

$$N\, R_{ee} = (1/k_{34}) + (1/k_{23}) + [k_{32}/(k_{23}\, k_{34})] + (1/k_{21}) + (1/k_{32}) + [k_{23}/(k_{32}\, k_{21})]$$

$$N\, R_{00} = (1/k_{14}) + (1/k_{41})$$

where N is the total amount of transporter. The maximum velocities and half-saturation constants characterizing the flux measurements under diverse experimental conditions, can be interpreted in terms of the relevant experimental parameters (Stein, 1986).

The expressions given in Eqs. (2) are determined by the detailed balance condition:

$$k_{12}\, k_{23}\, k_{34}\, k_{41} = k_{14}\, k_{43}\, k_{32}\, k_{21} \qquad (3)$$

From Eqs. (2), the SCM is characterized by the following property:

$$R_{ee} + R_{00} = R_{AB} + R_{BA} \qquad (4)$$

This property can be considered as a kinetic constraint for a SCM-like behavior (Stein, 1986; Hernández et al, 1996). Within the context of this work, I define as SCM-like behavior of a transporter the one where the unidirectional fluxes can be expressed in the form of Eqs. (1) and where the relevant experimental parameters are subject to the constraint represented by Eq. (4).

The General Carrier Model

The general carrier model (GCM) is shown in Fig. 2*A*. As can be seen, the connection between states 1–2 (and also between states 3–4) is via a single transitional step (like in the diagram of Fig. 1), representing the binding and release of L at the corresponding compartment. States 1–4 are connected via a complex network of transitional paths. Here I shall consider the case where states 1–4 are connected by an arrangement of parallel linear

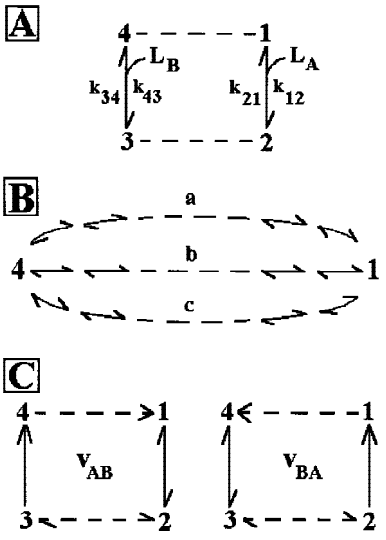

Fig. 2. (*A*) State diagram of the general carrier model. The transitions between states 1–2 and between states 3–4 are similar to the ones in the diagram of Fig. 1. States 1–4 and 2–3 are connected via a complex network of transitions. There is no binding and/or release of *L* to *A* or *B* at any of these transitions. (*B*) A particular case of the network connecting states 1–4, consisting of three parallel paths. In turn, each path consists of a linear sequence of individual transitions. (*C*) Cyclic diagrams representing the unidirectional fluxes v_{AB} and v_{BA}.

paths, each one consisting of a linear sequence of individual transitions (Fig. 2*B*). The same will apply for the connection between states 2–3. There are no additional paths connecting states 1–3 or states 2–4. There is no binding and/or release of *L* at any of the individual transitional steps belonging to the connection between states 1–4 or between states 2–3. I shall prove here that the GCM, represented by the diagram of Fig. 2*A* and embodied with the structural characteristics just described, exhibits relevant experimental parameters and restrictions formally analogous to the SCM (''SCM-like behavior,'' *see* previous section). In fact, the elementary SCM will be shown here to represent a particular case of the GCM. For the analysis, which is detailed in Appendices I and II, I employ the diagrammatic method (Hill, 1977). For the derivation of the unidirectional fluxes, I employ the cyclic diagrams shown in Fig. 2*C* (Hernández et al., 1996), which represent a condensed version of the ''expanded diagrams'' (Hill, 1989). Instead of considering the general case of *m* parallel paths per connection, which would obscure the basic arguments with overloaded algebra, I illustrate the demonstration for the particular case that each connection consists of three parallel paths (Fig. 2*B*).

Figure 3*A* shows, as an example, one of the linear paths belonging to connection 1–4 (path ''*a*''). Fig. 3*B* shows a graphical representation of the fundamental functions (arbitrarily called F^i, G^i, H^i and M^i) corresponding to the *i*th path in a connection, relevant for the

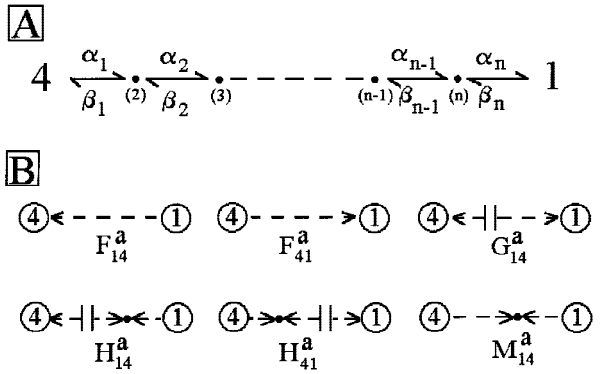

Fig. 3. (*A*) The structure of path ''*a*'' in connection 1–4, shown in detail. There are *n*–1 intermediate states inside the path, designated 2, 3, . . . , *n*–1. These should not be confused with the ''main'' states in the general carrier model (Fig. 2*A*). The αs and the βs are the pseudo-first order rate constants, governing the corresponding transitions inside the path. (*B*) Graphical representation of functions $F_{14}{}^a$, $F_{41}{}^a$, $G_{14}{}^a$, $H_{14}{}^a$, $H_{41}{}^a$, $M_{14}{}^a$. The following symbols denote: ⊣⊢, a single missing transition, ---> and <---, linear products of rate constants in the corresponding directions; -->●<--, linear product of rate constants converging to an intermediate state (●).

diagrammatic analysis of the GCM (shown also for path ''*a*'' in connection 1–4, in this case). In general, these functions are sums of products of pseudo-first order rate constants governing transitions belonging to the corresponding path. For the case of path ''*a*'' in connection 1–4, and assuming that this path contains n steps (Fig. 3*A*), the fundamental functions are given by

$$F_{41}{}^a = \alpha_1\alpha_2\alpha_3 \ldots \alpha_n;\ F_{14}{}^a = \beta_1\beta_2\beta_3 \ldots \beta_n$$

$$\begin{aligned} G_{14}{}^a = {} & \alpha_2\alpha_3 \ldots \alpha_n + \alpha_3\alpha_4 \ldots \alpha_n\beta_1 \\ & + \alpha_4\alpha_5 \ldots \alpha_n\beta_1\beta_2 + \ldots + \\ & + \alpha_{n-1}\,\alpha_n\beta_1\beta_2 \ldots \beta_{n-3} + \alpha_n\beta_1\beta_2 \ldots \beta_{n-2} \\ & + \beta_1\beta_2 \ldots \beta_{n-1} \end{aligned} \tag{5}$$

$$\begin{aligned} H_{41}{}^a = {} & \alpha_1\alpha_3\alpha_4 \ldots \alpha_n \\ & + \alpha_1(\alpha_2 + \beta_2)\alpha_4\alpha_5 \ldots \alpha_n \\ & + \alpha_1(\alpha_2\alpha_3 + \alpha_2\beta_3 + \beta_2\beta_3)\alpha_5\alpha_6 \ldots \alpha_n \\ & + \ldots + \\ & \alpha_1(\alpha_2\alpha_3 \ldots \alpha_{n-3} + \alpha_2\alpha_3 \ldots \alpha_{n-4}\beta_{n-3} + \ldots + \alpha_2\beta_3\beta_4 \\ & \ldots \beta_{n-3} + \beta_2\beta_3 \ldots \beta_{n-3})\alpha_{n-1}\alpha_n + \alpha_1(\alpha_2\alpha_3 \ldots \alpha_{n-2} \\ & + \alpha_2\alpha_3 \ldots \alpha_{n-3}\beta_{n-2} + \ldots + \alpha_2\beta_3\beta_4 \ldots \beta_{n-2} \\ & + \beta_2\beta_3 \ldots \beta_{n-2})\alpha_n \\ & + \\ & \alpha_1(\alpha_2\alpha_3 \ldots \alpha_{n-1} + \alpha_2\alpha_3 \ldots \alpha_{n-2}\beta_{n-1} \\ & + \ldots + \alpha_2\beta_3\beta_4 \ldots \beta_{n-1} + \beta_2\beta_3 \ldots \beta_{n-1}) \end{aligned}$$

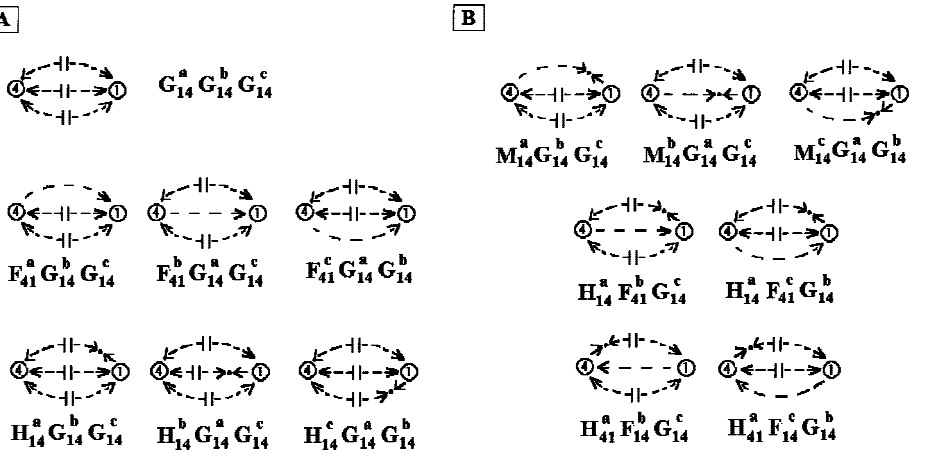

Fig. 4. Graphical representation of terms contained in functions G_{14}, F_{41}, and H_{14} (*A*) and in function M_{14} (*B*) (*see also* Fig. 3*B*).

$$
\begin{aligned}
H_{14}{}^{a} = {} & \beta_n\beta_1\beta_2 \ldots \beta_{n-2} \\
& + \\
& \beta_n(\alpha_{n-1} + \beta_{n-1})\beta_1\beta_2 \ldots \beta_{n-3} \\
& + \\
& \beta_n(\alpha_{n-2}\alpha_{n-1} + \alpha_{n-2}\beta_{n-1} + \beta_{n-2}\beta_{n-1})\beta_1\beta_2 \ldots \beta_{n-4} \\
& + \ldots + \\
& \beta_n(\alpha_4\alpha_5 \ldots \alpha_{n-1} + \alpha_4\alpha_5 \ldots \alpha_{n-2}\beta_{n-1} \\
& + \ldots + \alpha_4\beta_5\beta_6 \ldots \beta_{n-1} + \beta_4\beta_5 \ldots \beta_{n-1})\beta_1\beta_2 \\
& + \\
& \beta_n(\alpha_3\alpha_4 \ldots \alpha_{n-1} + \alpha_3\alpha_4 \ldots \alpha_{n-2}\beta_{n-1} \\
& + \ldots + \alpha_3\beta_4\beta_5 \ldots \beta_{n-1} + \beta_3\beta_5 \ldots \beta_{n-1})\beta_1 \\
& + \\
& \beta_n(\alpha_2\alpha_3 \ldots \alpha_{n-1} + \alpha_2\alpha_3 \ldots \alpha_{n-2}\beta_{n-1} \\
& + \ldots + \alpha_2\beta_3\beta_4 \ldots \beta_{n-1} + \beta_3\beta_4 \ldots \beta_{n-1}) \\
M_{14}{}^{a} = {} & \alpha_1\alpha_2 \ldots \alpha_{n-1}\beta_n + \alpha_1\alpha_2 \ldots \alpha_{n-2}\beta_{n-1}\beta_n \\
& + \ldots + \alpha_1\alpha_2\beta_3\beta_4 \ldots \beta_n + \alpha_1\beta_2\beta_3 \ldots \beta_n
\end{aligned}
\tag{5}
$$

In Eqs. (5), the αs and βs are the pseudo-first order rate constants governing the corresponding transitions (Fig. 3*A*). Notice that the subindex in each of these constants denotes a transition contained inside the linear path (Fig. 3*A*) whereas the subindex in the ''*F*'', ''*G*'', ''*H*'' and ''*M*'' functions refers to the original states in the GCM (Fig. 2*A*). Also notice that the *G* and *M* functions are independent of the direction and therefore are unique for each path, whereas the *F* and *H* functions are defined for each direction within a path.

From the functions defined for each path, expressions for the relevant functions characterizing the complete connection (e.g., F_{14}, F_{41}, G_{14}, H_{14}, H_{41} and M_{14}) can be obtained. From the above considerations, F_{14}, F_{41}, G_{14}, H_{14}, H_{41} and M_{14} (and also F_{23}, F_{32}, G_{23}, H_{23}, H_{32} and M_{23}) are independent from L_A and L_B. For the case of connection 1–4, and for three parallel paths (Fig. 2*B* and Fig. 4), these functions are given by

$$
\begin{aligned}
F_{14} &= F_{14}{}^{a}G_{14}{}^{b}G_{14}{}^{c} + F_{14}{}^{b}G_{14}{}^{a}G_{14}{}^{c} + F_{14}{}^{c}G_{14}{}^{a}G_{14}{}^{b} \\
F_{41} &= F_{41}{}^{a}G_{14}{}^{b}G_{14}{}^{c} + F_{41}{}^{b}G_{14}{}^{a}G_{14}{}^{c} + F_{41}{}^{c}G_{14}{}^{a}G_{14}{}^{b} \\
G_{14} &= G_{14}{}^{a}G_{14}{}^{b}G_{14}{}^{c} \\
H_{14} &= H_{14}{}^{a}G_{14}{}^{b}G_{14}{}^{c} + H_{14}{}^{b}G_{14}{}^{a}G_{14}{}^{c} + H_{14}{}^{c}G_{14}{}^{a}G_{14}{}^{b} \\
H_{41} &= H_{41}{}^{a}G_{14}{}^{b}G_{14}{}^{c} + H_{41}{}^{b}G_{14}{}^{a}G_{14}{}^{c} + H_{41}{}^{c}G_{14}{}^{a}G_{14}{}^{b} \\
M_{14} &= M_{14}{}^{a}G_{14}{}^{b}G_{14}{}^{c} + M_{14}{}^{b}G_{14}{}^{a}G_{14}{}^{c} + M_{14}{}^{c}G_{14}{}^{a}G_{14}{}^{b} + \\
&\quad + H_{14}{}^{a}(F_{41}{}^{b}G_{14}{}^{c} + F_{41}{}^{c}G_{14}{}^{b}) + H_{41}{}^{a}(F_{14}{}^{b}G_{14}{}^{c} \\
&\quad + F_{14}{}^{c}G_{14}{}^{b}) + \\
&\quad + H_{14}{}^{b}(F_{41}{}^{a}G_{14}{}^{c} + F_{41}{}^{c}G_{14}{}^{a}) \\
&\quad + H_{41}{}^{b}(F_{14}{}^{a}G_{14}{}^{c} + F_{14}{}^{c}G_{14}{}^{a}) + \\
&\quad + H_{14}{}^{c}(F_{41}{}^{a}G_{14}{}^{b} + F_{41}{}^{b}G_{14}{}^{a}) + H_{41}{}^{c}(F_{14}{}^{a}G_{14}{}^{b} \\
&\quad + F_{14}{}^{b}G_{14}{}^{a}) +
\end{aligned}
\tag{6}
$$

Analogous functions can be obtained for connection 2–3 (F_{23}, F_{32}, G_{23}, H_{23}, H_{32} and M_{23}). With the aid of functions F_{14}, F_{41}, G_{14}, H_{14}, H_{41}, M_{14}, F_{23}, F_{32}, G_{23}, H_{23}, H_{32} and M_{23}, the directional diagrams of the model can be classified into main groups, according to the position of the missing transition(s) and the state considered (Fig. 5). In previous work (Hernández & Fischbarg, 1994), we used a similar type of global diagrammatic analysis to study the general transport properties of a two-conformational single-file pore model with an arbitrary number of positions in the file. For the case under consideration, I made the kinetic analysis of the GCM in Appendix I. The proof that the restriction represented by Eq. (4) is satisfied by the GMC is given in Appendix II. Although the demonstration was done only for the case of the parellel-paths design, it is possible that it can be generalized to more complex structures (e.g., including connections between the paths). In the following section

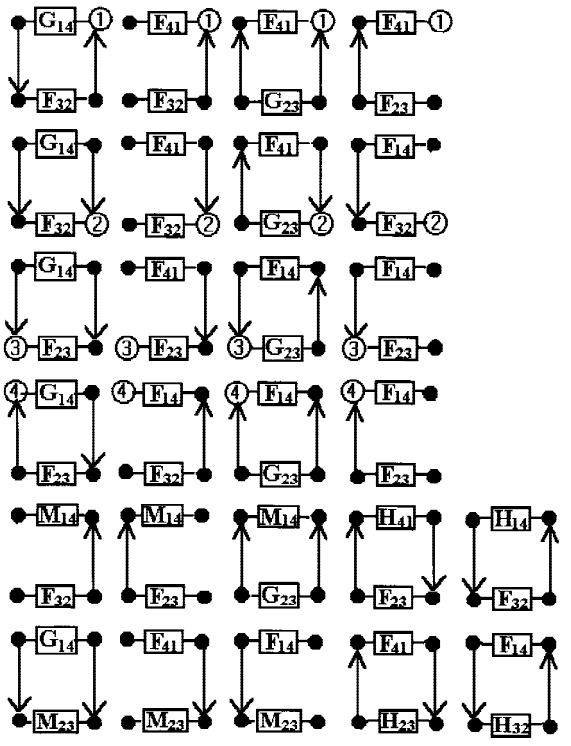

Fig. 5 General graphical representation of the directional diagrams of the model in Fig. 2. First four rows, from the upper to the lower row: representations corresponding to states 1, . . . , 4, respectively. Fifth and sixth rows: representations corresponding to the states contained inside connections 1–4 and 2–3, respectively.

I consider, as illustrations of the approach, some specific cases.

Particular Examples

The Simple Carrier Model

For the case of the SCM (Fig. 1), and considering the general definitions [Fig. 3*A* and *B*, Eqs. (5) and (6)],

$$\begin{aligned} &F_{14} = k_{14};\ F_{41} = k_{41};\ F_{23} = k_{23};\ F_{32} = k_{32} \\ &G_{14} = 1;\ G_{23} = 1 \\ &H_{14} = H_{41} = 0;\ H_{23} = H_{32} = 0 \\ &M_{14} = 0;\ M_{23} = 0 \end{aligned} \tag{7}$$

Substitution of the relations given by Eqs. (7) into the general expressions for the relevant experimental parameters [Eqs. (A5*b*)] permits one to obtain Eqs. (2). Hence, the SCM represents a particular case of the GCM.

Two-ligand Pore Model

Figure 6*A* shows the state diagram corresponding to a particular mechanism of a two-site pore capable of binding two ligands. In this case, the ligand (*L*) can bind the pore from each of the compartments only if the other ligand (*M*) is already bound to the countersite. Once inside the pore, *L* can jump between the two internal sites. *M* can only bind the pore when *L* is not already bound to it. The example is merely illustrative, and does not intend to describe any actual experimental situation.

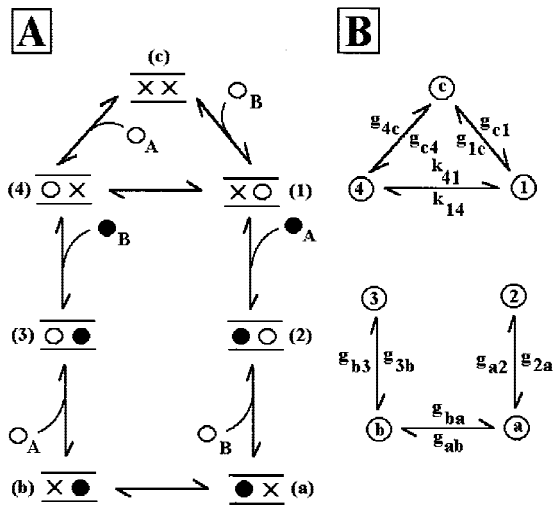

Fig. 6. (*A*) State diagram of a facilitative transporter mediating the passage of ligands *L* (dark circles) and *M* (clear circles) between compartments *A* and *B*. 1, 2, 3, 4, *a*, *b* and *c* are the intermediate states of the transporter. (*B*) A detailed representation of the paths connecting states 1–4 and 2–3. k_{14} and k_{41} are true first-order rate constants, the rest are pseudo-first order rate constants.

From the analysis of Fig. 6*B*, the following particular expressions are obtained for the relevant functions of connection 1–4:

$$\begin{aligned} &F_{14} = k_{14}(g_{c1} + g_{c4}) + g_{1c}g_{c4};\ F_{41} = k_{41}\,(g_{c1} + g_{c4}) + g_{4c}g_{c1} \\ &G_{14} = g_{c1} + g_{c4} \\ &H_{14} = g_{1c};\ H_{41} = g_{4c} \\ &M_{14} = g_{1c}g_{4c} + k_{14}g_{4c} + k_{41}g_{1c} \end{aligned} \tag{8a}$$

In addition, the following expressions are obtained for connection 2–3:

$$\begin{aligned} &F_{23} = g_{2a}g_{ab}g_{b3};\ F_{32} = g_{3b}g_{ba}g_{a2} \\ &G_{23} = g_{a2}g_{b3} + g_{ab}g_{b3} + g_{ba}g_{a2} \\ &H_{23} = g_{2a}(g_{ab} + g_{ba} + g_{b3}) \\ &H_{32} = g_{3b}(g_{ab} + g_{ba} + g_{a2}) \\ &M_{23} = g_{2a}g_{3b}(g_{ab} + g_{ba}) \end{aligned} \tag{8b}$$

In Eqs. (8*a*) and (8*b*), the *g*s are the pseudo-first order rate constants governing the transitions inside connec-

tions 1–4 and 2–3 (Fig. 6*B*). From Eqs. (8*a*) and (8*b*), the general relations given by Eqs. (A6*b*) are satisfied for this particular case. Therefore, the pore mechanism represented by Fig. 6*A* exhibits SCM-like behavior for the macroscopic kinetic properties characterizing the transport of *L*. This example is particularly illustrative, since the SCM-like behavior occurs in the absence of a translatory carrier mechanism or of conformational changes of the transporter.

Other Examples

In previous work (Hernández & Fischbarg, 1994; Hernández et al., 1996) we studied the properties of some transport systems characterized by complex kinetic diagrams. The state-diagram corresponding to the two-conformational single-file pore capable of binding two ligands (*w* and *L*), functioning under near-saturation conditions for an abundant ligand *w* (e.g., water) and under a single-occupancy regime for a second ligand L (Hernández & Fischbarg, 1994), accommodates well into the structural characteristics of the GCM (*see* Fig. 2). Although the relevant experimental parameters characterizing the transport of *L* were not explicitly derived for this case, the structural features of the state diagram permit one to predict that the two-conformational single-file pore exhibits SCM-like behavior. As mentioned above, in another example (Hernández et al., 1996), a two-site two-conformational pore binding a single ligand *L* was demonstrated to exhibit SCM-like behavior. The model describing this mechanism was also embodied with the general structural features characterizing the GCM (Fig. 2).

The basic idea underlying these models was that ligand movement through an inner protein channel represented a more realistic mechanism for facilitated transport than internal single-site displacement determined by conformational changes of the protein. In fact, complex channel-like mechanisms have been suggested to operate in diverse processes of mediated transport (for references, *see* Hernández & Fischbarg, 1994; Su et al., 1996). The concept that classical carriers and channels are particular cases of more general types of transport systems was first developed by Läuger (1980, 1984) and underlied diverse subsequent analysis (Berry & Edmonds, 1992; Chen & Eisenberg, 1993; Hernández & Fischbarg, 1994; Larsson et al., 1996; Su et al., 1996). The study performed here suggests that many facilitative transport systems operating via channel-like mechanisms are represented by kinetic diagrams that conform to the basic structural characteristics of the GCM, and would therefore exhibit SCM-like macroscopic behavior.

Conclusions

From the point of view of the kinetic analysis, the main contribution of this study is the generalization of the restrictions governing the relevant experimental parameters, previously determined for the particular case of the simple carrier model, to a general carrier model. The main result in this respect is that the general carrier model introduced here is also subject to analogous restrictions of its relevant experimental parameters. The basic conclusion of this work is therefore that there is a general kinetic design of a transporter that determines similar macroscopic properties to the ones of the simple carrier model.

From the above, the main conclusion of biological interest is that the finding of a SCM-like behavior for a complex facilitative transporter does not constitute a sufficient argument in favor of the four-state SCM. Correspondingly, that experimental evidence is not necessarily suggestive of a particular type of mechanism, like the classically invoked one involving conformational transitions between two states of a single-site transporter (Fig. 1). The underlying mechanism can be a more complex process described by a more involved kinetic scheme, and can even take place in the absence of conformational changes of the transporter.

This research was supported by the Comisión Sectorial de Investigación Cientifica de la Universidad de la República, and by the Programa para el Desarrollo de las Ciencias Básicas, Uruguay.

References

Andersen, O.S. 1989. Kinetics of ion movement mediated by carriers and channels. *Methods in Enzymology* **171:**62–112

Baldwin, S.A. 1993. Mammalian passive glucose transporters: members of an ubiquitous family of active and passive transport proteins. *Biochim. Biophys. Acta* **947:**571–590

Berry, R., Edmonds, D.T. 1992. Carrier-like behavior from a static but electrically responsive model pore. *J. Theor. Biol.* **154:**249–260

Carruthers, A. 1990. Facilitated diffusion of glucose. *Physiol. Rev.* **70:**1135–1176

Chen, D.P., Eisenberg, R.S. 1993. Flux, coupling, and selectivity in ionic channels of one conformation. *Biophys. J.* **65:**727–746

Gould, G.W., Holman, G.D. 1993. The glucose transporter family: structure, function and tissue-specific expression. *Biochem. J.* **295:**329–341

Hernández, J.A., Fischbarg, J. 1994. Transport properties of single-file pores with two conformational states. *Biophys. J.* **67:**996–1006

Hernández, J.A., Fischbarg, J., Vera, J.C. 1996. Modeling facilitative sugar transporters: transitions between single and double ligand occupancy of multiconformational channel models explain anomalous kinetics. *J. Membrane Biol.* **149:**57–69

Hill, T.L. 1977. Free Energy Transduction in Biology. Academic Press, New York

Hill, T.L. 1989. Free Energy Transduction and Biochemical Cycle Kinetics. Springer-Verlag, New York, 71–76

Krupka, R.M., Deves, R. 1981. An experimental test for cyclic versus linear transport models. The mechanism of glucose and choline transport in erythrocytes. *J. Biol. Chem.* **256:**5410–5416

Krupka, R.M., Deves, R. 1983. Kinetics of inhibition of transport systems. *Int. Rev. Cytol.* **84:**303–352

Larsson, H.P., Picaud, S.A., Werblin, F.S., H. Lecar. 1996. Noise

analysis of the glutamate-activated current in photoreceptors. *Biophys. J.* **70:**733–742

Läuger, P. 1980. Kinetic properties of ion carriers and channels. *J. Membrane Biol.* **57:**163–178

Läuger, P. 1984. Channels with multiple conformational states: interrelations with carriers and pumps. *In:* Current Topics in Membrane and Transport. F. Bronner and W.D. Stein, Editors. **21:**309–326. Academic, New York

Lieb, W.R., Stein, W.D. 1974. Testing and characterizing the simple carrier. *Biochim. Biophys. Acta* **373:**178–196

Schultz, S.G. 1980. Basic Principles of Membrane Transport. pp. 33–41, 85, 95, 96. Cambridge University Press, Cambridge

Stein, W.D. 1986. Transport and Diffusion across Cell Membranes. Academic Press, Orlando, Fl., 231–242

Stein, W.D. 1990. Channels, Carriers, and Pumps. An Introduction to Membrane Transport. pp. 154–164. Academic Press, San Diego, CA

Su, A., Mager, S., Mayo, S.L., Lester, H.A. 1996. A multi-substrate single-file model for ion-coupled transporters. *Biophys. J.* **70:**762–77

Walmsley, A.R. 1988. The dynamics of the glucose transporter. *Trends Biochem. Sci.* **13:**226–231

Wheeler, T.J., Whelan, T.D. 1988. Infinite-cis kinetics support the carrier model for erythrocyte glucose transport. *Biochemistry* **27:**1441–1450

Appendix I

Kinetic Analysis of the General Carrier Model

The sum of all the directional diagrams of the model shown in Fig. 2 (Σ) is given by

$$\Sigma = D_1 + D_2 + D_3 + D_4 + D_{14} + D_{23} \tag{A1a}$$

$D_1, \ldots, D_4$ are the sums of all the directional diagrams of states $1, \ldots, 4$, and D_{14} and D_{23} are the sums of all the directional diagrams of the states contained inside connections 1–4 and 2–3, respectively (Fig. 5). From Eqs. (5) and (6), these sums are given by

$$D_1 = F_{32}G_{14}k_{43}k_{21}L_B + F_{41}(G_{23}k_{34}k_{21} + F_{32}k_{21} + F_{23}k_{34})$$

$$D_2 = F_{32}G_{14}k_{43}k_{12}L_AL_B + F_{41}k_{12}(F_{32} + G_{23}k_{34})L_A + F_{14}F_{32}k_{43}L_B$$

$$D_3 = F_{23}G_{14}k_{43}k_{12}L_AL_B + F_{23}F_{41}k_{12}L_A + F_{14}k_{43}(F_{23} + G_{23}k_{21})L_B$$

$$D_4 = F_{23}G_{14}k_{34}k_{12}L_A + F_{14}(G_{23}k_{34}k_{21} + F_{32}k_{21} + F_{23}k_{34})$$

$$D_{14} = F_{23}H_{41}k_{12}k_{34}L_A + F_{32}H_{14}k_{43}k_{21}L_B + M_{14}(F_{23}k_{34} + F_{32}k_{21} + G_{23}k_{34}k_{21})$$

$$D_{23} = F_{41}H_{23}k_{12}k_{34}L_A + F_{14}H_{32}k_{43}k_{21}L_B + M_{23}(G_{14}k_{12}k_{43}L_AL_B + F_{41}k_{12}L_A + F_{14}k_{43}L_B) \tag{A1b}$$

From Eqs. (A1), Σ can also be expressed as

$$\Sigma = E_0 + E_1L_A + E_2L_B + E_3L_AL_B \tag{A2a}$$

with

$$E_0 = (F_{14} + F_{41} + M_{14})(F_{23}k_{34} + F_{32}k_{21} + G_{23}k_{34}k_{21})$$

$$E_1 = [F_{23}k_{34}(G_{14} + H_{41}) + F_{41}(F_{23} + F_{32} + G_{23}k_{34} + H_{23}k_{34} + M_{23})]k_{12}$$

$$E_2 = [F_{32}k_{21}(G_{14} + H_{14}) + F_{14}(F_{23} + F_{32} + G_{23}k_{21} + H_{32}k_{21} + M_{23})]k_{43}$$

$$E_3 = (F_{23} + F_{32} + M_{23})G_{14}k_{12}k_{43} \tag{A2b}$$

The detailed balance condition requires that

$$k_{12}F_{23}k_{34}F_{41} = F_{14}k_{43}F_{32}k_{21} \tag{A3}$$

The unidirectional fluxes v_{AB} and v_{BA} (in the $A \rightarrow B$ and $B \rightarrow A$ directions, respectively) can be derived from the cyclic diagrams shown in Fig. 2*C* (Hernández et al., 1996). They are given by

$$v_{AB} = (T_1L_A + T_3L_AL_B)/\Sigma$$
$$v_{BA} = (T_2L_B + T_3L_AL_B)/\Sigma \tag{A4a}$$

where, from the detailed balance restriction [Eq. (A3)],

$$T_1 = T_2 = Nk_{12}F_{23}k_{34}F_{41} = NF_{14}k_{43}F_{32}k_{21}$$
$$T_3 = (1/T_1)(F_{32}k_{43}k_{21})/[F_{41}(F_{23}k_{34} + F_{32}k_{21} + G_{23}k_{34}k_{21})] \tag{A4b}$$

The relevant experimental parameters K, R_{00}, R_{ee}, R_{AB} and R_{BA} (Lieb & Stein, 1974; Stein, 1986) can be expressed in terms of the parameters E_0, E_1, E_2, E_3, T_1 and T_3 as follows (Hernández et al, 1996):

$$K = T_1/T_3;\ KR_{00} = E_0/T_1;$$
$$R_{AB} = E_1/T_1;\ R_{BA} = E_2/T_1;\ R_{ee}/K = E_3/T_1. \tag{A5a}$$

From Eqs. (A2*b*, A4*b* and A5*a*), the relevant experimental parameters characterizing the GMC are given by

$$K = (F_{41}/G_{14})[1/k_{43}) + F_{23}k_{34}/(F_{32}k_{43}k_{21}) + G_{23}k_{34}/(F_{32}k_{43})]$$

$$NR_{00} = [G_{14}(F_{14} + F_{41} + M_{14})]/(F_{14}F_{41})$$

$$NR_{AB} = (1/k_{34}) + [(F_{32} + M_{23})/(F_{23}k_{34})] + [(G_{14} + H_{41})/F_{41}] + [(G_{23} + H_{23})/F_{23}]$$

$$NR_{BA} = (1/k_{21}) + [(F_{23} + M_{23})/(F_{32}k_{21})] + [(G_{14} + H_{14})/F_{14}] + [(G_{23} + H_{32})/F_{32}]$$

$$NR_{ee} = (1/k_{34}) + [(F_{32} + M_{23})/(F_{23}k_{34})] + (1/k_{21}) + + [(F_{23} + M_{23})/(F_{23}k_{21})] + (G_{23}/F_{32}) + (G_{23}/F_{23}) + F_{23}M_{23}/(F_{23}F_{32}) \tag{A5b}$$

where N is the total amount of transporter. From Eqs. (A5*b*), the necessary and sufficient condition to satisify the kinetic restriction given by Eq. (4) (that is, $R_{ee} + R_{00} = R_{AB} + R_{BA}$) is

$$(H_{14}/F_{14}) + (H_{41}/F_{41}) + (H_{32}/F_{32}) + (H_{23}/F_{23}) = G_{14}M_{14}/(F_{14}F_{41}) + G_{23}M_{23}/(F_{23}F_{32}) \tag{A6a}$$

In order to demonstrate that Eq. (A6*a*) is satisfied, it is sufficient to prove that, simultaneously,

$$F_{14}H_{41} + F_{41}H_{14} = G_{14}M_{14}$$

and

$$F_{23}H_{32} + F_{32}H_{23} = G_{23}M_{23} \tag{A6b}$$

Since both connections (between states 1–4 and states 2–3) have similar structures, it is sufficient to prove that Eq. (A6*b*) is satisified for any one of the connections. The proof that Eq. (A6*b*) is satisfied is sketched in Appendix II, for the case that connection 1–4 consists of three parallel linear paths (Fig. 2*B*). Since the structure of each connection is

generalizable to any number of parallel paths, the demonstration remains valid for the general case.

Appendix II

Proof that $F_{14}H_{41} + F_{41}H_{14} = G_{14}M_{14}$

Linear Path Theorem

From Eqs. (6) and Fig. 4,

$$F_{14}H_{41} + F_{41}H_{14} = (F_{14}{}^{a}H_{41}{}^{a} + F_{41}{}^{a}H_{14}{}^{a})(G_{14}{}^{b}G_{14}{}^{c})^2 + (F_{14}{}^{b}H_{41}{}^{b} + F_{41}{}^{b}H_{14}{}^{b})(G_{14}{}^{a}G_{14}{}^{c})^2 + (F_{14}{}^{c}H_{41}{}^{c} + F_{41}{}^{c}H_{14}{}^{c})(G_{14}{}^{a}G_{14}{}^{b})^2 + \text{cross terms}$$

and

$$G_{14}M_{14} = (G_{14}{}^{a}M_{14}{}^{a})(G_{14}{}^{b}G_{14}{}^{c})^2 + (G_{14}{}^{b}M_{14}{}^{b})(G_{14}{}^{a}G_{14}{}^{c})^2 + (G_{14}{}^{c}M_{14}{}^{c})(G_{14}{}^{a}G_{14}{}^{b})^2 + \text{cross terms} \quad \text{(A7)}$$

with

$$\text{cross terms} = G_{14} \times [G_{14}{}^{c}(F_{14}{}^{a}H_{41}{}^{b} + F_{41}{}^{a}H_{14}{}^{b} + F_{14}{}^{b}H_{41}{}^{a} + F_{41}{}^{b}H_{14}{}^{a}) + G_{14}{}^{b}(F_{14}{}^{a}H_{41}{}^{c} + F_{41}{}^{a}H_{14}{}^{c} + F_{14}{}^{c}H_{41}{}^{a} + F_{41}{}^{c}H_{14}{}^{a}) + G_{14}{}^{a}(F_{14}{}^{b}H_{41}{}^{c} + F_{41}{}^{b}H_{14}{}^{c} + F_{14}{}^{c}H_{41}{}^{b} + F_{41}{}^{c}H_{14}{}^{b})]$$

From Eqs. (A7), it only remains to be proved that, for each path i(i = $a, b, c, \ldots$),

$$F_{14}{}^{i}H_{41}{}^{i} + F_{41}{}^{i}H_{14}{}^{i} = G_{14}{}^{i}M_{14}{}^{i} \quad \text{(A8)}$$

Since all the paths have a similar structure (linear sequence of transitions governed by pseudo-first order rate constants independent of L_A and L_B), it is sufficient to prove that, for instance, Eq. (A8) is satisfied by path ''a'' (Fig. 3*A*). In what follows, I sketch the demonstration that this is indeed the case (Linear path theorem).

I express $H_{14}{}^{a}$ and $H_{41}{}^{a}$ [Eqs. (5)] as

$$H_{14}{}^{a} = h_{14}{}^{2} + h_{14}{}^{3} + \ldots + h_{14}{}^{n}$$
$$H_{41}{}^{a} = h_{41}{}^{2} + h_{41}{}^{3} + \ldots + h_{41}{}^{n} \quad \text{(A9}a\text{)}$$

where the superindex denotes the corresponding state inside path ''a'' (Fig. 3*A*). Thus, for instance, for state ''2'' inside the path,

$$h_{41}{}^{2} = \alpha_1 \times [\alpha_3\alpha_4 \ldots \alpha_n + \alpha_4\alpha_5 \ldots \alpha_n\beta_2 + \alpha_5\alpha_6 \ldots \alpha_n\beta_2\beta_3 + \ldots + \alpha_{n-1}\alpha_n\beta_2\beta_3 \ldots \beta_{n-3} + \alpha_n\beta_2\beta_3 \ldots \beta_{n-2} + \beta_2\beta_3 \ldots \beta_{n-1}]$$

$$h_{14}{}^{2} = \beta_2\beta_3 \ldots \beta_n \quad \text{(A9}b\text{)}$$

Analogously, each term in $M_{14}{}^{a}$ [Eqs. (5)] corresponds to each state inside path ''a'':

$$M_{14}{}^{a} = m_{14}{}^{2} + m_{14}{}^{3} + \ldots + m_{14}{}^{n} \quad \text{(A10}a\text{)}$$

Thus, for instance,

$$m_{14}{}^{2} = \alpha_1\beta_2\beta_3 \ldots \beta_n \quad \text{(A10}b\text{)}$$

From Eqs (5), (A9) and (A10),

$$G_{14}{}^{a}m_{14}{}^{2} = \alpha_1\beta_1\beta_2 \ldots \beta_n \times [\alpha_3\alpha_4 \ldots \alpha_n + \alpha_4\alpha_5 \ldots \alpha_n\beta_2 + \alpha_5\alpha_6 \ldots \alpha_n\beta_2\beta_3 + \ldots + \alpha_{n-1}\alpha_n\beta_2\beta_3 \ldots \beta_{n-3} + \alpha_n\beta_2\beta_3 \ldots \beta_{n-2} + \beta_2\beta_3 \ldots \beta_{n-1}] + + \alpha_1\alpha_2 \ldots \alpha_n\beta_2\beta_3 \ldots \beta_n = = F_{14}{}^{a}h_{41}{}^{2} + F_{41}{}^{a}h_{14}{}^{2} \quad \text{(A11)}$$

The relation given by Eq. A(11) can be generalized to every state inside the path. Hence, from Eqs. (5), (A9)–(A11), $G_{14}{}^{a}M_{14}{}^{a} = F_{14}{}^{a}H_{41}{}^{a} + F_{41}{}^{a}H_{14}{}^{a}$.